



**HAL**  
open science

## The N-terminal domain of TET1 promotes the formation of dense chromatin regions refractory to transcription

Audrey Lejart, Siham Zentout, Catherine Chapuis, Ostiane D'augustin,  
Rebecca Smith, Gilles Salbert, Sébastien Huet

### ► To cite this version:

Audrey Lejart, Siham Zentout, Catherine Chapuis, Ostiane D'augustin, Rebecca Smith, et al.. The N-terminal domain of TET1 promotes the formation of dense chromatin regions refractory to transcription. *Chromosoma*, 2022, 131 (1-2), pp.47-58. 10.1007/s00412-022-00769-0 . hal-03613049v1

**HAL Id: hal-03613049**

**<https://hal.science/hal-03613049v1>**

Submitted on 16 May 2022 (v1), last revised 18 May 2022 (v2)

**HAL** is a multi-disciplinary open access archive for the deposit and dissemination of scientific research documents, whether they are published or not. The documents may come from teaching and research institutions in France or abroad, or from public or private research centers.

L'archive ouverte pluridisciplinaire **HAL**, est destinée au dépôt et à la diffusion de documents scientifiques de niveau recherche, publiés ou non, émanant des établissements d'enseignement et de recherche français ou étrangers, des laboratoires publics ou privés.



Distributed under a Creative Commons Attribution - NonCommercial 4.0 International License



**HAL**  
open science

## The N-terminal domain of TET1 promotes the formation of dense chromatin regions refractory to transcription

Audrey Lejart, Siham Zentout, Catherine Chapuis, Ostiane D'augustin,  
Rebecca Smith, Gilles Salbert, Sébastien Huet

### ► To cite this version:

Audrey Lejart, Siham Zentout, Catherine Chapuis, Ostiane D'augustin, Rebecca Smith, et al.. The N-terminal domain of TET1 promotes the formation of dense chromatin regions refractory to transcription. *Chromosoma*, Springer Verlag, 2022, 131 (1-2), pp.47-58. 10.1007/s00412-022-00769-0 . hal-03613049

**HAL Id: hal-03613049**

**<https://hal.archives-ouvertes.fr/hal-03613049>**

Submitted on 16 May 2022

**HAL** is a multi-disciplinary open access archive for the deposit and dissemination of scientific research documents, whether they are published or not. The documents may come from teaching and research institutions in France or abroad, or from public or private research centers.

L'archive ouverte pluridisciplinaire **HAL**, est destinée au dépôt et à la diffusion de documents scientifiques de niveau recherche, publiés ou non, émanant des établissements d'enseignement et de recherche français ou étrangers, des laboratoires publics ou privés.



Distributed under a Creative Commons Attribution - NonCommercial | 4.0 International License

# The N-terminal domain of TET1 promotes the formation of dense chromatin regions refractory to transcription

Audrey Lejart<sup>1</sup>, Siham Zentout, Catherine Chapuis<sup>1</sup>, Ostiane d'Augustin, Rebecca Smith<sup>1</sup>, Gilles Salbert<sup>1,#</sup> and Sébastien Huet<sup>1,2#</sup>

1 Univ Rennes, CNRS, IGDR (Institut de Génétique et Développement de Rennes) - UMR 6290, BIOSIT (Biologie, Santé, Innovation Technologique de Rennes) - UMS 3480, US 018, F-35000 Rennes, France

2 Institut Universitaire de France, Paris, France

#Correspondence:

G.S. : Tel: +33 2 23 23 66 25; Email: gilles.salbert@univ-rennes1.fr

S.H. : Tel: +33 2 23 23 45 57; Email: sebastien.huet@univ-rennes1.fr

## ABSTRACT

### Background

The methylated form of cytosine, 5-methylcytosine, is an epigenetic mark found at CpG dinucleotides and associated with transcription silencing. TET (Ten-eleven translocation) enzymes initiate active cytosine demethylation via the oxidation of 5-methylcytosine. Due to its role in transcription, the TET family, and in particular its founding member TET1, has been implicated in multiple processes such as cell differentiation, tumorigenesis and neurodegeneration. TET1 is composed of a C-terminal domain, which bears the catalytic activity of the enzyme, and a N-terminal region that is less well characterized except for the CXXC domain responsible for the targeting to CpG islands. While TET1-induced cytosine demethylation promotes transcription, this protein is also known to interact with chromatin regulating factors that rather silence this process, with the coordination between these two opposite functions of TET1 being unclear.

### Results

In the present work, we uncover a new function of the N-terminal domain of the TET1 protein in the regulation of the chromatin architecture. This domain of the protein promotes the establishment of a compact chromatin architecture displaying reduced turnover of core histones and partial eviction of the histone linker. This chromatin reorganisation process, which does not rely on the CXXC domain, is associated with a global shut-down of transcription and an increase in heterochromatin associated histone epigenetic marks.

### Conclusions

Based on our findings, we propose that the N-terminal domain of TET1, which strongly associates with chromatin, could either promote the recruitment of chromatin factors involved in chromatin condensation, or directly favour chromatin unmixing from the nucleoplasm. The dense chromatin

organisation generated by the N-terminal domain of TET1 could contribute to restrain the transcription enhancement induced by the DNA demethylation activity of this enzyme.

## KEYWORDS

Ten Eleven translocation enzyme, DNA methylation, DNA hydroxymethylation, chromatin, transcription, fluorescence microscopy.

## INTRODUCTION

In the nucleus of eukaryotic cells, DNA is wrapped around histones to form the chromatin fibre which, itself, displays a hierarchy of folding steps. The complex organization of chromatin is essential to ensure that the entire genetic material of the cell can be contained within the nucleus, where it occupies 20 to 50% of the nuclear volume [1]. Despite this high level of packaging, the chromatin structure is not fixed and constantly evolves in relation to multiple cellular processes which require access to DNA such as transcription, replication or repair [2]. Key actors in the regulation of chromatin folding are epigenetic marks such as post-transcriptional modifications found on histones and base modifications found in DNA. These dynamic marks attract or repel effectors of DNA transactions and control chromatin organisation either directly, by modulating for example nucleosome stability, or indirectly, by recruiting remodelers or chromatin scaffolding proteins [3].

While epigenetic marks found on histones are extremely diverse, only a handful of modifications are found at the DNA level, the main one being 5-methylcytosine (5-mC) [4]. This mark, mainly found at CpG dinucleotides, has a repressive impact on transcription, in particular through the recruitment of repressor complexes and by regulating the binding of transcription factors to DNA at regulatory regions [5,6]. 5-mC is written by several DNA methyl-transferase enzymes and its removal arises either by passive dilution due to DNA replication or by active DNA demethylation [7,8]. The main active demethylation pathway is based on the successive oxidation of 5-mC into 5-hmC (5-hydroxymethylcytosine), 5-fC (5-formylcytosine) and finally 5-caC (5-carboxylcytosine), which are carried out by members of the TET (ten-eleven translocation) enzyme family [9]. While the 5-fC and 5-caC forms are rapidly excised by the DNA repair machinery to restore an unmethylated cytosine [10], 5-hmC has a relatively long lifetime and could thus constitute a fully-fledged epigenetic mark [11].

The TET family is composed of three members showing distinct expression patterns hinting at different cellular functions [12]. All members share a catalytic domain responsible for 5-mC oxidation that is localized at the C-terminus of the proteins [13,14]. Furthermore, TET1 and TET3, but not TET2, bear a CXXC domain that binds to unmethylated CpGs and is thought to be

responsible for the localization of these proteins at CpG-rich genomic sites like CpG islands, protecting them from aberrant methylation [13]. By controlling the balance of 5-mC/5-hmC levels within the genome, the TET enzymes are key regulators of transcriptional processes associated with cell differentiation, tumorigenesis and neurodegeneration [15,16]. However, the role of TET enzymes is not limited to their catalytic activity. Indeed, they have been shown to serve as a binding platform for effectors that regulate transcription such as the histone methyltransferase complex PRC2 [17], the histone acetyltransferase hMOF [18] or the O-linked N-acetylglucosamine transferase OGT [19,20]. Importantly, the existence of a shorter isoform of TET1 (TET1<sub>short</sub>) has been recently reported. While the long isoform of TET1 (TET1<sub>long</sub>) is expressed mainly in undifferentiated cells, TET1<sub>short</sub> levels seem to increase upon differentiation as well as during tumorigenesis [21,22]. Despite lacking the N-terminal domain of TET1<sub>long</sub>, including the CXXC domain, TET1<sub>short</sub> is still able to demethylate CpG islands [22]. Nevertheless, TET1<sub>short</sub> cannot fully complement the longer isoform, suggesting that the N-terminal domain of the full-length protein fulfils specific cellular functions that remain to be clarified.

In the present work, we demonstrate that the N-terminal region of the TET1 protein, which is lacking in TET1<sub>short</sub>, is able to induce a global reorganisation of chromatin. This restructuring process is seen at the larger chromatin folding scales but also at the molecular level since histone turnover is impacted by the TET1 N-terminal domain. We also show that the chromatin reorganisation is associated with a global shut-down of transcription. Altogether, our findings uncover a previously unidentified function of TET1 in the regulation of the chromatin structure with potential consequences regarding its roles in the regulation of transcription.

## RESULTS

### **Ectopic expression of TET1 leads to a global reorganisation of the chromatin structure**

By using confocal fluorescence imaging, we observed that ectopic expression of TET1 and TET2, but not TET3, led to a global reorganisation of the chromatin within the nucleus of human osteosarcoma U2OS cells (Fig. 1a). While the chromatin in control cells, as shown by Hoechst staining, occupied the entire nuclear space relatively evenly, the expression of TET1 and TET2 led to an unmixing of the nucleus content, with chromatin condensing into large bundles and some nuclear areas largely devoided of staining. Since this phenotype was more pronounced for TET1, we focused on the impact of TET1 expression on chromatin structure. To better understand how chromatin reorganisation arises upon the TET1 ectopic expression, we transiently transfected GFP-tagged TET1 or free GFP in U2OS cells stably expressing H2B-mCherry and monitored the progressive increase in the GFP fluorescence levels in parallel with changes in the fluorescence

contrast of the chromatin pattern, used as a readout of the chromatin compaction state in living cells. While no significant change in the chromatin pattern was observed in cells expressing GFP (Fig. S1), a rapid increase of the fluorescence contrast was observed upon expression of TET1-GFP (Fig. 1b,c). The tight correlation between the timing of the chromatin reorganisation and the rising of TET1 levels within the nucleus suggests that the change in the chromatin pattern is directly linked to the presence of TET1 rather than a secondary consequence of cellular mechanisms controlled by this enzyme.

TET1 is responsible for 5-mC oxidation to allow its later replacement by unmethylated cytosine [13]. However, when expressing a catalytically inactive form of TET1 we observed the same chromatin pattern as with the wild-type enzyme (Fig 1d). Furthermore, this reorganisation phenotype also did not rely on the CXXC domain of TET1 (Fig 1d). Therefore, these data show that the change in chromatin structure promoted by TET1 is not the consequence of 5-mC oxidation processes or further DNA demethylation steps.

### **The N-terminal domain of TET1 is sufficient to induce chromatin reorganisation**

To better delineate the domains of TET1 responsible for chromatin reorganisation, we analysed the impact of the expression of two truncated forms of the full-length protein: a C-terminal fragment (CTER) bearing the catalytic domain shared between the different TET proteins, and a N-terminal fragment (NTER) which remains poorly characterized except for the CXXC domain (Fig 2a). Importantly, the CTER is reminiscent of the recently identified short isoform of TET1 found expressed in differentiated cells. While the CTER is still able to oxidize 5-mC into 5-hmC, in line with what is reported for TET1<sub>short</sub> (Fig S2), its expression in U2OS cells did not lead to visible changes in the chromatin organisation (Fig 2b). In contrast, expression of the NTER fragment, while not affecting 5-hmC levels within the nucleus (Fig S2), led to a global reorganisation of the chromatin similar to what was observed with the full-length protein (Fig 2b). Importantly, this chromatin restructuring phenotype upon expression of the NTER fragment was also observed in human HeLa and MCF-7 cells, demonstrating that it is not specific to U2OS cells (Fig 2c).

We also assessed the affinity of these two truncated TET1 constructs for chromatin by monitoring the kinetics of fluorescence recovery after photobleaching (FRAP) for each GFP tagged construct. Although the NTER fragment appeared less bound to chromatin than the full length TET1, it displayed a much slower recovery than the CTER construct (Fig 2d-f), confirming previous findings showing that it is principally the NTER region that controls TET1 binding to chromatin [22]. Noteworthy, despite their major impact on chromatin organisation, both the full length TET1 and the NTER still displayed a rapid turnover at chromatin, with characteristic exchange times of few seconds.

Altogether, these results demonstrate that the dynamic association of the N-terminal domain of TET1 with chromatin alters higher-order chromatin states, as shown by light microscopy, ultimately leading to a spatial redistribution of the genomic material within the nucleus.

### **Large-scale chromatin reorganisation promoted by the N-terminal domain of TET1 is associated with changes in histone turnover**

We next assessed whether the changes in chromatin folding induced by the N-terminal domain of TET1 were also associated with altered dynamics of its molecular constituents. Histones are key chromatin scaffolding proteins regulating the spatial organization of the genome within the nucleus, and their turnover correlates with the chromatin compaction state [23,24]. Therefore, we assessed the impact of the N-terminal domain of TET1 on the exchange rates of two different histones: the core histone H2B as well as the linker histone H1. Using fluorescence recovery after photobleaching (FRAP), we observed that expression of the N-terminal domain of TET1 decreased H2B turnover (Fig 3a,b), in line with the fact that this domain seems to promote the local condensation of chromatin. Conversely, the linker histone H1 displayed higher exchange rates in cells expressing the N-terminal domain of TET1 compared to controls (Fig 3c,d). Therefore, the dense chromatin domains generated by the expression of the N-terminal domain of TET1 differs from transcriptionally silent heterochromatic areas in which H1 displays increased binding [23,24].

### **Expression of the N-terminal domain of TET1 leads to a global shutdown of transcription**

The results obtained so far demonstrate that the N-terminal domain of TET1 regulates the architecture of chromatin at multiple scales. Since this enzyme was shown to play key roles in the regulation of transcription, we next tested whether the changes in chromatin organisation induced by the N-terminal domain of TET1 were also associated with a modulation of the transcriptional state. We used 5-ethynyl uridine (EU) staining to measure the level of nascent RNAs in cells expressing the N-terminal domain of TET1 and observed that this domain not only led to a global reduction in nascent RNA levels but also seemed to confine transcription at the interface between the dense chromatin domains and the nucleoplasm (Fig 4a,b). Concomitantly to this reduction in RNA synthesis rates, we also found that the presence of this domain of TET1 led to a global increase in the levels of trimethylation of the lysine 27 of histone H3 (H3K27me3), an epigenetic mark written by PCR2 and found within facultative heterochromatin [25] (Fig 4c,d). Altogether, these findings demonstrate that the N-terminal domain of TET1 is able to shut-down transcription by establishing a chromatin environment displaying some of the characteristics found in heterochromatin regions.

## DISCUSSION

Our data show that ectopic expression of TET1 promotes chromatin remodeling leading to the establishment of a condensed chromatin architecture refractory to transcription. The dense chromatin domains observed in the presence of TET1 seems to demix from the nucleoplasm. They share some features found in heterochromatin, such as increased levels of H3K27me3 [26], but nevertheless differ from these compact regions. Indeed, while the histone linker H1 was shown to be crucial for the condensation of the chromatin fibre [27], the compact chromatin conformation promoted by TET1 tend to rather exclude this histone. Interestingly, senescence associated heterochromatin foci, which arise from heterochromatic areas detaching from the nuclear lamina, also show H1 eviction due to its replacement by the high mobility group protein A2 (HMGA2) [28]. It would be useful to assess whether TET1 ectopic expression could promote cell senescence.

The TET1-mediated chromatin condensation process reported here is independent of both the catalytic activity of this enzyme and its targeting to CpG islands via the CXXC domain. The N-terminal region of the protein, which triggers this condensation, displays a strong affinity for chromatin. Therefore, it could serve as a platform to recruit factors modulating chromatin conformation, as it was recently proposed for OGT [22]. TET1 has been shown to interact with the histone-deacetylases Sin3A and HDAC1 as well as the chromatin remodeler CHD4, three actors known to promote chromatin compaction [19]. The recruitment of these proteins to chromatin due to their binding to TET1 may therefore contribute to the establishment of the compact genome organisation observed in cells expressing the N-terminal domain of TET1. Furthermore, the increase in H3K27me3 staining in these dense domains may be promoted by the association between TET1 and the PRC2 complex [29], contributing to a global silencing of transcription. Interestingly, analyzing the sequence of the N-terminal domain of TET1 predicts that it contains several disordered stretches covering about 70% of the domain length (Fig. S3) [30]. These disordered regions are known to promote phase demixing in the cellular environment, a process that has been proposed to regulate the formation of multiple functional domains within the nucleus [31,32]. Therefore, the binding of the partially disordered N-terminal domain of TET1 to chromatin may favour its demixing from the rest of nucleoplasm, leading to the formation of chromatin bundles reminiscent the initial steps of chromosome individualisation during prophase.

## CONCLUSIONS

In this work, we uncovered a new role of the N-terminal region of TET1 in the regulation of the chromatin organisation and transcription inhibition. The inhibitory impact of this region of the protein might be needed to balance the positive influence of the catalytic domain on transcription, where unrestrained activity of the recently identified short isoform of TET1 is associated with

tumorigenesis [21]. Further work will be needed to better delineate the characteristics of this coordination mechanism between the two domains of TET1.

## **METHODS**

### **Plasmids**

The full length GFP-TET1, GFP-TET2 and GFP-TET3 plasmids are gifts from Heinrich Leonhardt and Cristina Cardoso [33]. The plasmids of the GFP tagged C-terminal and N-terminal fragments of TET1 as well as the GFP tagged mutant lacking the CXXC domain were provided by Wei Xie [22]. The catalytically-inactive mutant of full length TET1 fused to GFP was obtained by direct mutagenesis on GFP-TET1 with primers 5'- gttgtgcatgttgtaatggccttgtaagaatgggcacaaaaatcc-3' and 5'- ggattttgtgccattcttacaaggccattcacaacatgcacaac-3' using Phusion polymerase (Thermo Scientific). The GFP-NLS plasmid was provided by Haico Van Attikum [34]. The H2B-mCherry was a gift from Jan Ellenberg (Euroscarf P30632, [35]). mEGFP was cut from H1-mEGFP (gift from Gyula Timinszky) and replaced with mCherry using the restriction sites BshTI and Bsp1407I (ThermoScientific), to generate the H1-mCherry construct.

### **Cell culture**

All cell lines were cultured in DMEM (4.5 g/L glucose, Sigma) supplemented with 10% fetal bovine serum (Life Technologies), 2 mM glutamine (Sigma), 100 µg/mL penicillin and 100 U/mL streptomycin (Sigma) in a humidified incubator at 37 °C with 5% CO<sub>2</sub>. For transient expression of fluorescent constructs, cells were transfected 5 hours after seeding into glass-bottom chambers (Thermo Scientific and Zell Contact) with XtremeGENE HP (Roche) or Xfect (Takara Bio) according to the manufacturer's instructions and incubated for 24 hours prior to imaging. U2OS stably expressing H2B-mCherry were generated by transfection of the H2B-mCherry plasmid followed by a two week selection in growing medium supplemented with puromycin (0.25µg/ml, Invivogen) for 2 weeks. Immediately prior imaging live cells, growth medium was replaced with CO<sub>2</sub>-independent imaging medium (Phenol Red-free Leibovitz's L-15 medium (Life Technologies) supplemented with 20% fetal bovine serum, 2 mM glutamine, 100 µg/mL penicillin and 100 U/mL streptomycin). All experiments were completed with unsynchronized cells.

### **Immunofluorescence staining**

Cells were fixed using 4% paraformaldehyde and permeabilized with 0.1% Triton X-100 at room temperature. For 5-hmC staining, chromatin was denatured by adding hydrochloric acid at 2 M for 30min. Cells were blocked with BSA 3% Tween 0.05% solution in PBS before incubation overnight at 4°C with primary antibodies recognizing 5-hmC (Active Motif, ref 39769) or the

trimethylation of histone H3 at lysine 27 (Upstate, ref 07-449), diluted in the blocking buffer. The secondary antibodies labeled with Alexa Fluor 555 (ThermoScientific, ref A21428) diluted in the blocking buffer was added for one hour at room temperature. DNA was stained for 15 min with Hoechst 3342 at 1 µg/mL (ThermoScientific).

### **Nascent RNA staining by 5-ethynyl uridine**

For nascent RNA staining, cells were incubated with 5-ethynyl uridine (EU) at 1 mM in culture medium for 1 h before being fixed with 4% paraformaldehyde. Cells were permeabilised with 0.1% Triton X-100 for 15 min before RNA was labeled using the Click-iT® RNA Alexa Fluor® 594 Imaging Kit according to the manufacturer's instructions.

### **Confocal imaging and fluorescence recovery after photobleaching**

Fluorescence imaging of live and fixed cells was on a LSM880 point-scanner confocal microscope (Zeiss) using a 60x/1.4 N.A. oil-immersion objective lens. The fluorescence of the different fluorescent proteins or organic dyes used to stain the cell samples were excited with the most appropriate laser lines and detection was performed on the GaAsP detector array, choosing detection windows adapted to the emission spectrum of each fluorophore. The pixel size was set to 70 nm. FRAP of H2B-mCherry was performed on the same setup. Half of the nucleus was bleached at 561 nm and cells were imaged for 8 h at 1 image per hour to monitor the progressive recovery within the bleached area. FRAP of H1-mCherry as well as the full-length or truncated forms of TET1 tagged with GFP was completed on a Ti-E inverted microscope from Nikon equipped with a CSU-X1 spinning-disk head from Yokogawa, a Plan APO 60x/1.4 N.A. oil-immersion objective lens and a sCMOS ORCA Flash 4.0 camera. A circle of 4 µm diameter within the nucleus was bleached at 561 or 488 nm and fluorescence recovery was followed by imaging the cells for 25 to 50 seconds at 4 frames/second. For all live-cell experiments, cells were maintained at 37°C with a heating chamber.

### **Image analysis**

Image analysis was performed using the ImageJ software. For the quantification of fluorescence signals, the mean intensity within manually defined region delineating the nucleus was measured and subtracted from background. To monitor changes in the chromatin pattern, we estimated the fluorescence contrast on images of nuclei expressing H2B-mCherry, using the plugin GLCM\_Texture written by Julio E. Cabrera. The characteristic radius used to estimate this contrast was set to 10 pixels, which correspond to the characteristic size of the chromatin domains generated by the ectopic expression of TET1. For each timelapse acquisition of a single nucleus, the

chromatin contrast was estimated in parallel to the level of expression of unfused GFP or TET1-GFP, assessed by the mean intensity in the GFP channel. The expression level was then rescaled to range between 0 and 1. Before averaging, the individual curves for the chromatin contrast and the expression level were aligned in time using as a reference the timepoint at which the normalized expression level equaled to 0.5.

To analyze the FRAP acquisitions, regions of interest were defined manually to measure the fluorescence intensities within the bleached area ( $I_{bleach}$ ), the whole nucleus ( $I_{nuc}$ ) and outside the cell ( $I_{bg}$ ), along the entire image sequence. Based on these intensity measurements, the intensity within the bleached area was corrected from background and from the loss of total nuclear intensity due to both local photobleaching and timelapse imaging [36], using the following expression:

$$I_{frap} = \frac{I_{bleach} - I_{bg}}{I_{nuc} - I_{bg}}$$

After subtracting the signal estimated immediately after the bleach, the intensity was normalized to the signal pre bleach.

## Statistics

For the curves displaying time courses, means±SD are shown. Boxplots were generated using a web-tool developed by the Tyers and Rappsilber labs (<http://boxplot.tyerslab.com/>). The box limits correspond to the 25th and 75th percentiles and the bold line indicates the median value. The whiskers extend 1.5 times the interquartile range and outliers are shown by dots. p values were calculated using either two-sided unpaired Student's t-test assuming unequal variances for data showing normal distributions, or unpaired two-samples Wilcoxon test. On the boxplots, \* refers to p<0.05, \*\* to p<0.01, \*\*\* to p<0.001, \*\*\*\* to p<0.0001 and n.s. to non significant.

## LIST OF ABBREVIATIONS

5-caC: 5-carboxylcytosine

5-fC: 5-formylcytosine

5-mC: 5-methylcytosine

5-hmC: 5-hydroxymethylcytosine

EU: 5-ethynyl uridine

FRAP: fluorescence recovery after photobleaching

GFP: green fluorescent protein

H3K27me3: trimethylation of lysine 27 from histone H3

OGT: O-linked N-acetylglucosamine transferase

TET: ten-eleven translocation

## **DECLARATIONS**

### **Ethics approval and consent to participate**

Not applicable

### **Consent for publication**

Not applicable

### **Availability of data and materials**

The raw datasets used during the current study are available from the corresponding authors on reasonable request.

### **Competing interests**

The authors declare no competing interests.

### **Funding**

This work was funded by the Ligue contre le Cancer du Grand-Ouest, the Conseil Régional de Bretagne and the Institut Universitaire de France.

### **Authors' contributions**

A.L. and R.S. completed the experiments within the manuscript. C.C. generated cell lines and DNA constructs. G.S. and S.H. conceived and supervised this study. S.H. wrote the manuscript. All authors read and commented on the manuscript.

### **Acknowledgements**

We thank the engineers of the Microscopy Rennes Imaging Center (BIOSIT, Université Rennes 1), Stéphanie Dutertre and Xavier Pinson for technical assistance. This work would not have been possible without the generous donation of plasmids from Heinrich Leonhardt, Cristina Cardoso, Wei Xie, Haico Van Attikum, Gyula Timinszky and Jan Ellenberg.

## **REFERENCES**

1. Ou HD, Phan S, Deerinck TJ, Thor A, Ellisman MH, O'Shea CC. ChromEMT: Visualizing 3D chromatin structure and compaction in interphase and mitotic cells. *Science*. 2017;357.
2. Fierz B, Poirier MG. Biophysics of Chromatin Dynamics. *Annu Rev Biophys*. 2019;48:321–45.

3. Talbert PB, Henikoff S. Histone variants on the move: substrates for chromatin dynamics. *Nat Rev Mol Cell Biol.* 2017;18:115–26.
4. Rausch C, Hastert FD, Cardoso MC. DNA Modification Readers and Writers and Their Interplay. *J Mol Biol.* 2019;
5. Watt F, Molloy PL. Cytosine methylation prevents binding to DNA of a HeLa cell transcription factor required for optimal expression of the adenovirus major late promoter. *Genes Dev.* 1988;2:1136–43.
6. Iguchi-Ariga SM, Schaffner W. CpG methylation of the cAMP-responsive enhancer/promoter sequence TGACGTCA abolishes specific factor binding as well as transcriptional activation. *Genes Dev.* 1989;3:612–9.
7. Bhutani N, Burns DM, Blau HM. DNA Demethylation Dynamics. *Cell.* 2011;146:866–72.
8. Mulholland CB, Nishiyama A, Ryan J, Nakamura R, Yiğit M, Glück IM, et al. Recent evolution of a TET-controlled and DPPA3/STELLA-driven pathway of passive DNA demethylation in mammals. *Nat Commun.* 2020;11:5972.
9. Ito S, Shen L, Dai Q, Wu SC, Collins LB, Swenberg JA, et al. Tet proteins can convert 5-methylcytosine to 5-formylcytosine and 5-carboxylcytosine. *Science.* 2011;333:1300–3.
10. Maiti A, Drohat AC. Thymine DNA glycosylase can rapidly excise 5-formylcytosine and 5-carboxylcytosine: potential implications for active demethylation of CpG sites. *J Biol Chem.* 2011;286:35334–8.
11. Münzel M, Globisch D, Carell T. 5-Hydroxymethylcytosine, the sixth base of the genome. *Angew Chem Int Ed Engl.* 2011;50:6460–8.
12. Lorsbach RB, Moore J, Mathew S, Raimondi SC, Mukatira ST, Downing JR. TET1, a member of a novel protein family, is fused to MLL in acute myeloid leukemia containing the t(10;11) (q22;q23). *Leukemia.* 2003;17:637–41.
13. Tahiliani M, Koh KP, Shen Y, Pastor WA, Bandukwala H, Brudno Y, et al. Conversion of 5-methylcytosine to 5-hydroxymethylcytosine in mammalian DNA by MLL partner TET1. *Science.* 2009;324:930–5.
14. Hu L, Li Z, Cheng J, Rao Q, Gong W, Liu M, et al. Crystal structure of TET2-DNA complex: insight into TET-mediated 5mC oxidation. *Cell.* 2013;155:1545–55.
15. Rasmussen KD, Helin K. Role of TET enzymes in DNA methylation, development, and cancer. *Genes Dev.* 2016;30:733–50.
16. Jin S-G, Zhang Z-M, Dunwell TL, Harter MR, Wu X, Johnson J, et al. Tet3 Reads 5-Carboxylcytosine through Its CXXC Domain and Is a Potential Guardian against Neurodegeneration. *Cell Rep.* 2016;14:493–505.
17. Wu H, D'Alessio AC, Ito S, Xia K, Wang Z, Cui K, et al. Dual functions of Tet1 in transcriptional regulation in mouse embryonic stem cells. *Nature.* 2011;473:389–93.
18. Zhong J, Li X, Cai W, Wang Y, Dong S, Yang J, et al. TET1 modulates H4K16 acetylation by controlling auto-acetylation of hMOF to affect gene regulation and DNA repair function. *Nucleic Acids Res.* 2017;45:672–84.

19. Shi F-T, Kim H, Lu W, He Q, Liu D, Goodell MA, et al. Ten-eleven translocation 1 (Tet1) is regulated by O-linked N-acetylglucosamine transferase (Ogt) for target gene repression in mouse embryonic stem cells. *J Biol Chem.* 2013;288:20776–84.
20. Bauer C, Göbel K, Nagaraj N, Colantuoni C, Wang M, Müller U, et al. Phosphorylation of TET Proteins Is Regulated via O-GlcNAcylation by the O-Linked N-Acetylglucosamine Transferase (OGT) \*. *J Biol Chem.* 2015;290:4801–12.
21. Good CR, Madzo J, Patel B, Maegawa S, Engel N, Jelinek J, et al. A novel isoform of TET1 that lacks a CXXC domain is overexpressed in cancer. *Nucleic Acids Res.* 2017;45:8269–81.
22. Zhang W, Xia W, Wang Q, Towers AJ, Chen J, Gao R, et al. Isoform Switch of TET1 Regulates DNA Demethylation and Mouse Development. *Mol Cell.* 2016;64:1062–73.
23. Misteli T, Gunjan A, Hock R, Bustin M, Brown DT. Dynamic binding of histone H1 to chromatin in living cells. *Nature.* 2000;408:877–81.
24. Bancaud A, Huet S, Daigle N, Mozziconacci J, Beaudouin J, Ellenberg J. Molecular crowding affects diffusion and binding of nuclear proteins in heterochromatin and reveals the fractal organization of chromatin. *EMBO J.* 2009;28:3785–98.
25. Cao R, Wang L, Wang H, Xia L, Erdjument-Bromage H, Tempst P, et al. Role of histone H3 lysine 27 methylation in Polycomb-group silencing. *Science.* 2002;298:1039–43.
26. Wiles ET, Selker EU. H3K27 methylation: a promiscuous repressive chromatin mark. *Curr Opin Genet Dev.* 2017;43:31–7.
27. Willcockson MA, Heaton SE, Weiss CN, Bartholdy BA, Botbol Y, Mishra LN, et al. H1 histones control the epigenetic landscape by local chromatin compaction. *Nature.* 2021;589:293–8.
28. Funayama R, Saito M, Tanobe H, Ishikawa F. Loss of linker histone H1 in cellular senescence. *J Cell Biol.* 2006;175:869–80.
29. Neri F, Incarnato D, Krepelova A, Dettori D, Rapelli S, Maldotti M, et al. TET1 is controlled by pluripotency-associated factors in ESCs and downmodulated by PRC2 in differentiated cells and tissues. *Nucleic Acids Res.* 2015;43:6814–26.
30. Romero P, Obradovic Z, Kissinger C, Villafranca JE, Dunker AK. Identifying disordered regions in proteins from amino acid sequence. *Proc Int Conf Neural Netw ICNN97.* 1997. p. 90–5 vol.1.
31. Strom AR, Emelyanov AV, Mir M, Fyodorov DV, Darzacq X, Karpen GH. Phase separation drives heterochromatin domain formation. *Nature.* 2017;547:241–5.
32. Boehning M, Dugast-Darzacq C, Rankovic M, Hansen AS, Yu T, Marie-Nelly H, et al. RNA polymerase II clustering through carboxy-terminal domain phase separation. *Nat Struct Mol Biol.* 2018;25:833–40.
33. Frauer C, Rottach A, Meilinger D, Bultmann S, Fellingner K, Hasenöder S, et al. Different binding properties and function of CXXC zinc finger domains in Dnmt1 and Tet1. *PLoS One.* 2011;6:e16627.

34. Rother MB, Pellegrino S, Smith R, Gatti M, Meisenberg C, Wiegant WW, et al. CHD7 and 53BP1 regulate distinct pathways for the re-ligation of DNA double-strand breaks. *Nat Commun.* 2020;11:5775.
35. Neumann B, Walter T, Hériché J-K, Bulkescher J, Erfle H, Conrad C, et al. Phenotypic profiling of the human genome by time-lapse microscopy reveals cell division genes. *Nature.* 2010;464:721–7.
36. Bancaud A, Huet S, Rabut G, Ellenberg J. Fluorescence perturbation techniques to study mobility and molecular dynamics of proteins in live cells: FRAP, photoactivation, photoconversion, and FLIP. *Cold Spring Harb Protoc.* 2010;2010:pdb.top90.

## FIGURE LEGENDS

**Figure 1. The ectopic expression of TET1 leads to chromatin reorganisation.** **a.** Images of Hoechst-labeled UO2S cells expressing either unfused GFP, or GFP-tagged TET1, TET2 or TET3. **b.** Timelapse image sequence of live U2OS cells stably expressing H2B-mCherry and transiently expressing TET1-GFP. The images were pseudocolored according to the look-up table displayed on the right. **c.** Images from b. were quantified to monitor the changes in TET1-GFP expression levels (black curve), assessed by GFP fluorescence intensity, in parallel to the chromatin spatial distribution, assessed by the fluorescence contrast estimated from the images of the H2B-mCherry signal (red curve). The curves show a mean of 17 cells. **d.** Images of Hoechst-labeled U2OS cells expressing either unfused GFP, or wild-type TET1 (FL), a catalytically-inactive mutant of TET1 (FLmut) or a TET1 construct lacking the CXXC domain ( $\Delta$ CXXC), all tagged with GFP. For panels a., b. and d., scale bars = 10 $\mu$ m.

**Figure 2. The N-terminal domain of TET1 promotes chromatin reorganisation.** **a.** Schematic representation of TET1 protein domains. Cys-rich corresponds to a cysteine-rich region and DSBH stands for double-stranded  $\beta$ -helix. **b.** Images of Hoechst-labeled U2OS cells expressing either unfused GFP, full-length (FL), N-terminal domain (NTER) or C-terminal domain (CTER) of TET1, all tagged with GFP. **c.** Images of Hoechst-labeled HeLa and MCF-7 cells expressing unfused GFP or the N-terminal of TET1 tagged with GFP. **d.** Image sequences of the fluorescence redistribution after photobleaching a circular area of the nucleus (dotted red circles) of U2OS cells expressing either GFP fused to a nuclear localisation sequence (GFP-NLS), full-length TET1 (FL), the N-terminal domain of the protein (NTER) or its C-terminal domain (CTER), all tagged with GFP. **e.** Image from d. were quantified to assess the fluorescence recovery within the bleached region **f.** Levels of fluorescence recovery within the bleached area at 10 s after photobleaching estimated from the curves shown on panel e. 15 to 20 cells were acquired for each condition. For panels b. to d., scale bars = 10 $\mu$ m.

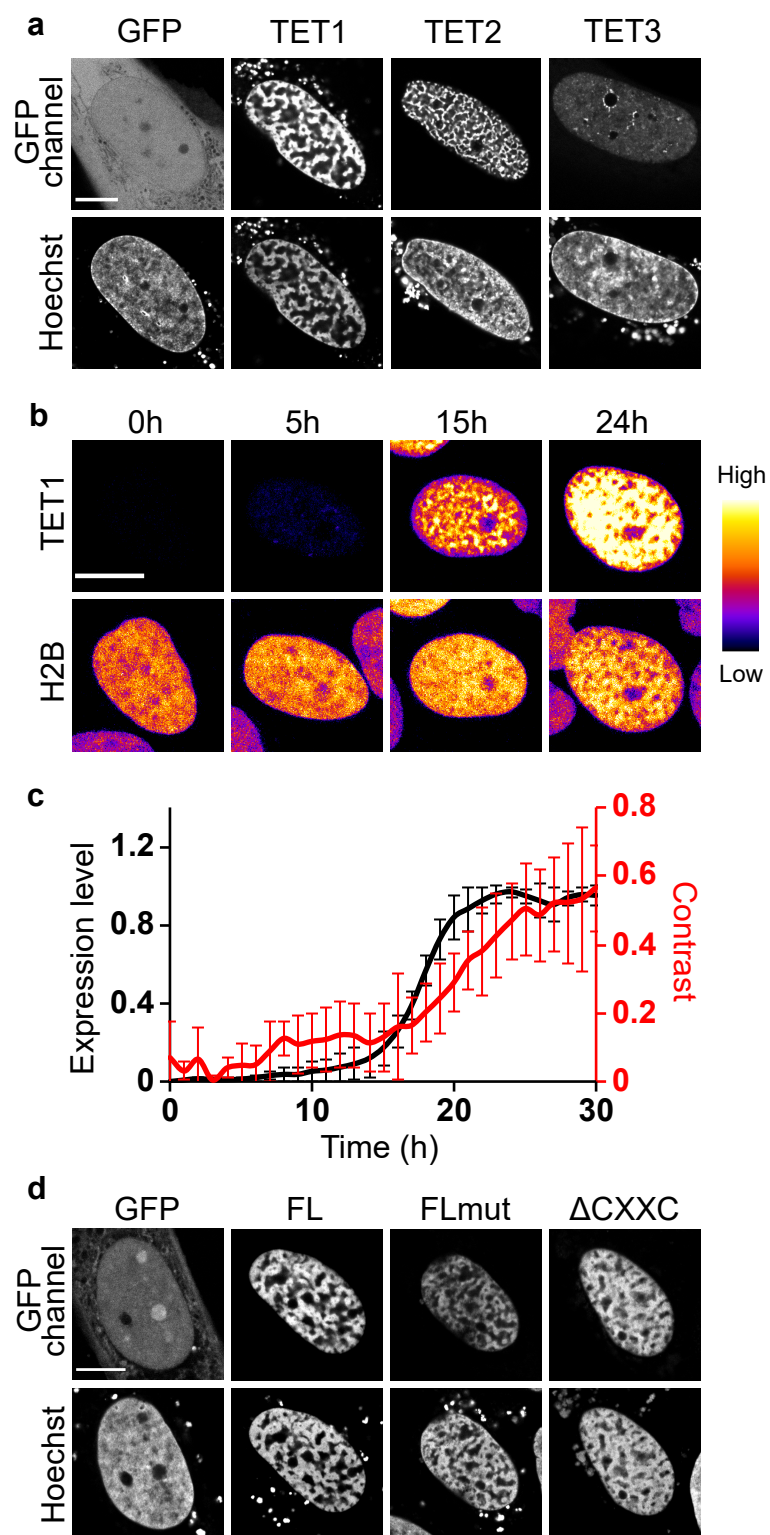
**Figure 3. The N-terminal domain of TET1 affects the turnover of histones H1 and H2B.** **a.** Image sequences of the fluorescence redistribution after photobleaching of the mCherry signal within half of the nucleus (dotted red outlines) of U2OS cells expressing H2B-mCherry together with either unfused GFP or the N-terminal domain of TET1 (NTER) tagged with GFP. **b.** Images from a. were quantified to assess the fluorescence recovery within the bleached region (left) as well as the levels of fluorescence recovery within the bleached area at 4h after photobleaching (right). 10 and 14 cells were acquired for the unfused GFP control and the NTER condition, respectively. **c.** Image sequences of the fluorescence redistribution after photobleaching of the mCherry signal within a circular area of the nucleus (dotted red circles) of U2OS cells expressing H1-mCherry together with either unfused GFP or the N-terminal domain of the protein (NTER) tagged with GFP. **d.** Images from e. were quantified to assess the fluorescence recovery within the bleached region (left) as well as the levels of fluorescence recovery within the bleached area at 10s after photobleaching (right). 18 and 17 cells were acquired for the unfused GFP control and the NTER condition, respectively. For panels a. and c., scale bars = 10 $\mu$ m.

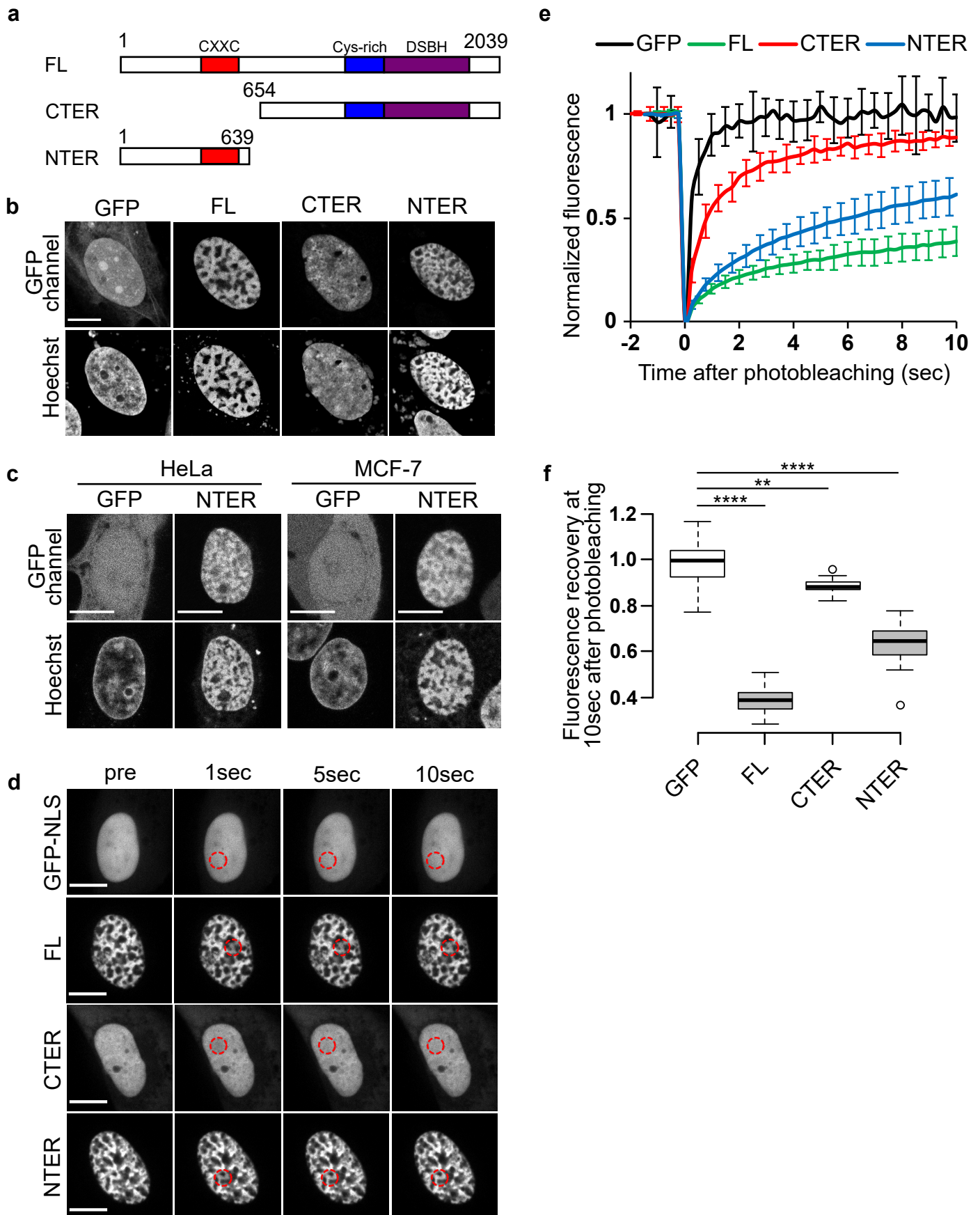
**Figure 4. The N-terminal domain of TET1 promotes transcription shut-down and H3K37me3 enrichment** **a.** Images of Hoechst-labeled U2OS cells expressing either unfused GFP, full-length (FL) or the N-terminal domain of TET1 (NTER), both tagged with GFP. The levels of nascent RNA were monitored by EU staining. **b.** Images from a. were quantified to estimate the mean nuclear levels of EU staining in each condition. Fluorescence signal was measured for more than 100 cells for each condition. **c.** Images of Hoechst-labeled U2OS cells expressing either unfused GFP, full-length (FL) or the N-terminal domain of TET1 (NTER), both tagged with GFP. The cells were also immunostained for the H3K27me3 histone mark. **b.** Images from c. were quantified to estimate the mean nuclear levels of H3K27me3 in each condition. Fluorescence signal was measured for more than 100 cells for each condition. For panels a. and c., scale bars = 10 $\mu$ m.

**Supplementary Figure 1. Control of the changes in chromatin compaction state upon expression of unfused GFP.** **a.** Timelapse image sequence of live U2OS cells stably expressing H2B-mCherry and transiently expressing unfused GFP. The images were pseudocolored according to the look-up table displayed on the right. **b.** Images from a. were quantified to monitor the changes in GFP expression levels (black curve), assessed by GFP fluorescence intensity, in parallel to the chromatin spatial distribution, assessed by the fluorescence contrast estimated from the images of the H2B-mCherry signal (red curve). The curves show a mean of 11 cells.

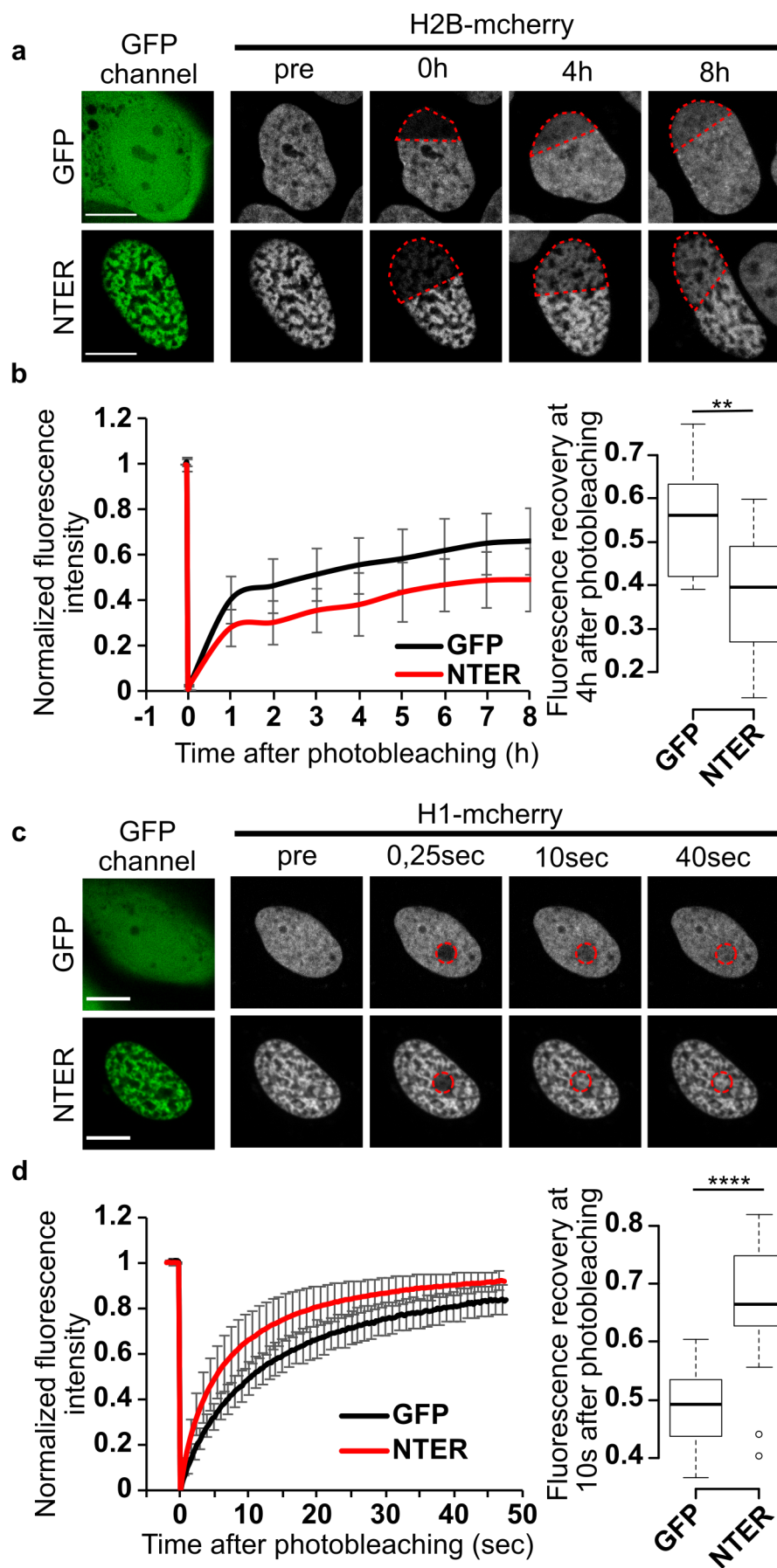
**Supplementary Figure 2. Influence of the N-terminal and C-terminal domains of TET1 on the levels of 5-hmC.** Images of Hoechst-labeled UO2S cells expressing either unfused GFP, full-length TET1 (FL), the C-terminal domain of TET1 (CTER) or the N-terminal domain of TET1 (NTER), all tagged with GFP. The cells were also immunostained for 5-hmC.

**Supplementary Figure 3. Prediction of the presence of disordered regions within the N-terminal domain of TET1.** The presence of disordered stretches was assessed with the PONDR software (<http://www.pondr.com>), using the VL-XT predictor. Levels of disorder above 0.5 corresponds to high probabilities of disordered regions.

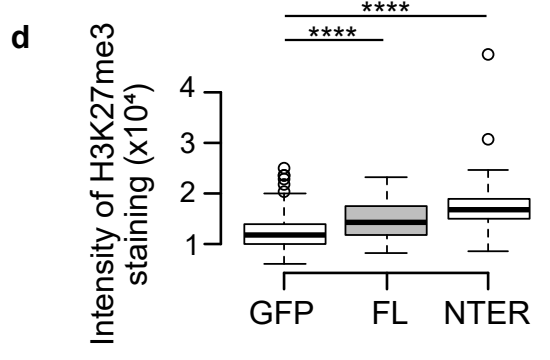
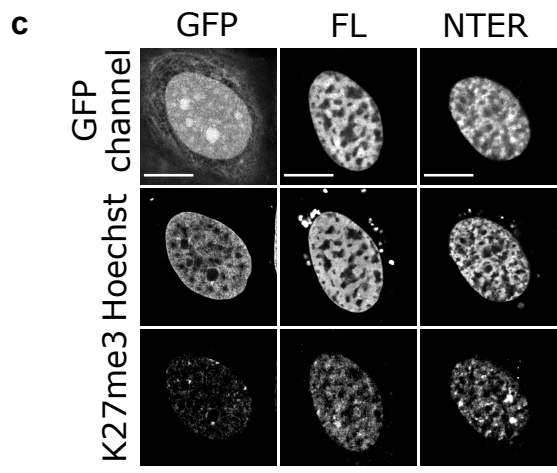
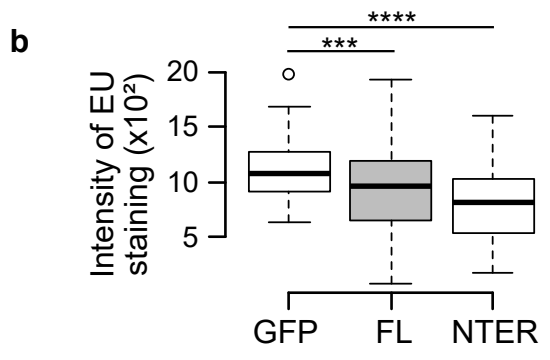
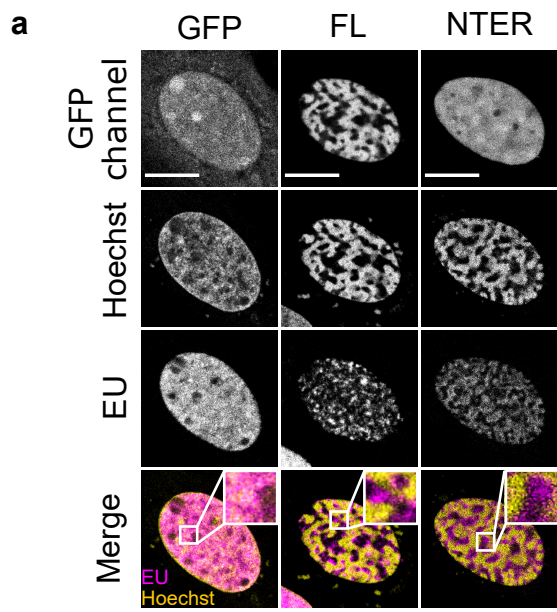




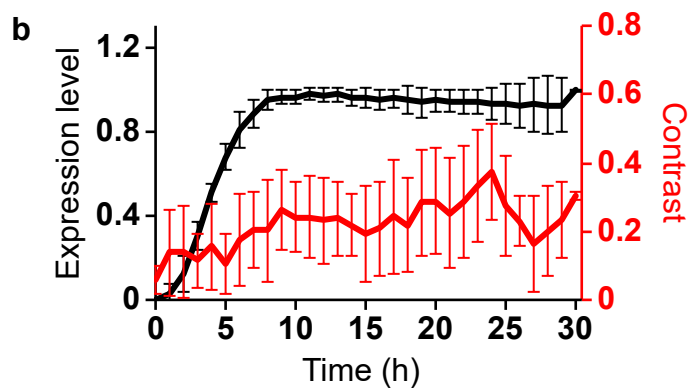
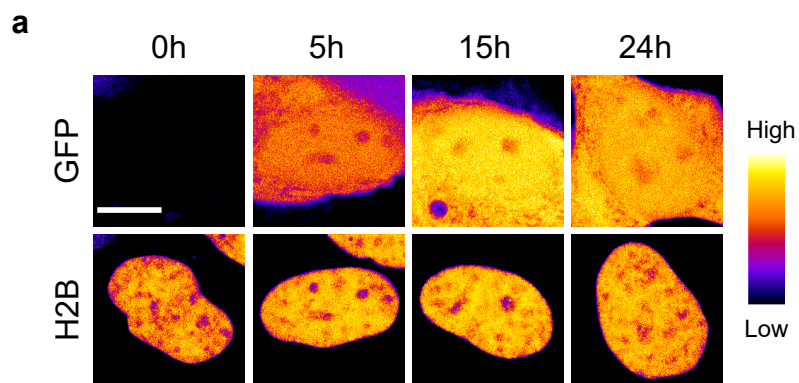
Lejart et al., Figure 2.

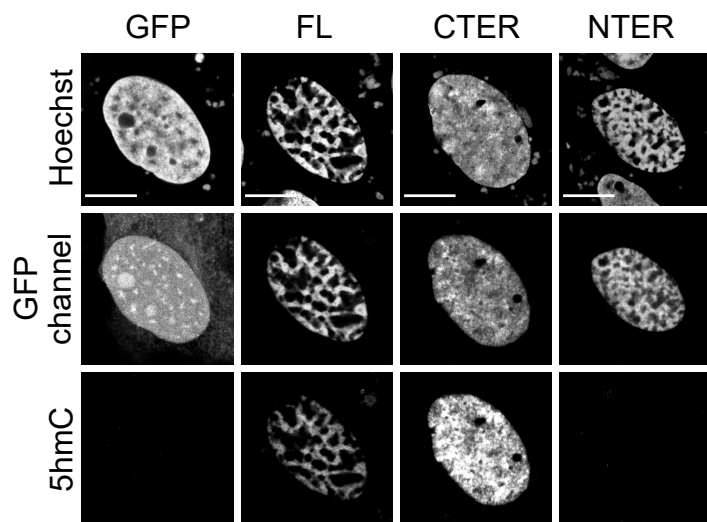


Lejart et al., Figure 3.

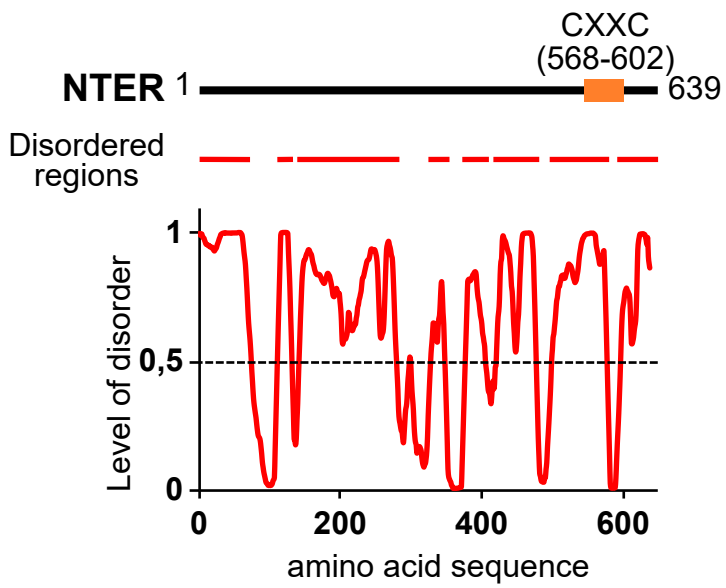


Lejart et al., Figure 4.





Lejart et al., Supplementary figure 2.



Lejart et al., Supplementary Figure 3.